VOL. 107 NO. WW4. NOV. 1981

# JOURNAL OF THE WATERWAY PORT COASTAL AND OCEAN DIVISION

PROCEEDINGS OF
THE AMERICAN SOCIETY
OF CIVIL ENGINEERS

AMERICAN SOCIETY OF CIVIL ENGINEERS FOUNDED 1852

VOL. 107 NO. WW4. NOV. 1981

# JOURNAL OF THE WATERWAY PORT COASTAL AND OCEAN DIVISION

PROCEEDINGS OF
THE AMERICAN SOCIETY
OF CIVIL ENGINEERS

Charles B. Chesnutt, Editor
U.S. Army Coastal Engineering
Research Center


ISSN 0148-9895

# CONTENTS



TECHNICAL NOTES

Proc. Paper 16621



The Journal of the Waterway, Port, Coastal and Ocean Division (ISSN 0148-9895) is published quarterly by the American Society of Civil Engineers. Publications office is at 345 East 47th Street, New York, N.Y. 10017. Address all ASCE correspondence to the Editorial and General Offices at 345 East 47th Street, New York, N.Y. 10017. Allow six weeks for change of address to become effective. Subscription price to members is $8.00. Nonmember subscriptions available; prices obtainable on request. Second-class postage paid at New York, N.Y. and at additional mailing offices. WW.

POSTMASTER: Send address changes to American Society of Civil Engineers, 345 East 47th Street, New York, NY 10017.

## DISCUSSION

Proc. Paper 16620



### INFORMATION RETRIEVAL

The key words, abstract, and reference "cards" for each article in this Journal represent part of the ASCE participation in the EJC information retrieval plan. The retrieval data are placed herein so that each can be cut out, placed on a 3 × 5 card and given an accession number for the user's file. The accession number is then entered on key word cards so that the user can subsequently match key words to choose the articles he wishes. Details of this program were given in an August, 1962 article in CIVIL ENGINEERING, reprints of which are available on request to ASCE headquarters.

## STATEMENT OF OWNERSHIP

The *Journal of the Waterway, Port, Coastal and Ocean Division* is edited and published by the American Society of Civil Engineers, with general business offices at 345 East 47th Street, New York, N.Y. 10017. The Manager of Technical and Professional Publications is Richard R. Torrens.

This Journal is owned wholly by the American Society of Civil Engineers, a nonprofit educational and professional organization with about 78,000 members. There are no individual owners or stockholders.

| | Average No. Copies Each Issue During Preceding 12 Months | Single Issue Nearest To Filing Date |
|---|---|---|
| Total no. copies printed (net press run) | 5,906 | 5,782 |
| Paid mail circulation | 4,183 | 4,419 |
| Sales through dealers and counter sales | None | None |
| Free distribution | None | None |
| Total distribution | 4,183 | 4,419 |
| Left Over (extra for new orders, office use, etc.) | 1,723 | 1,363 |
| Total | 5,906 | 5,782 |

*I certify that the above statements made by me are correct and complete.—Richard R. Torrens, Manager of Technical and Professional Publications.*

## 16632 DEEP WATER RENEWAL IN SUBARCTIC FJORD

KEY WORDS: **Alaska;** Fjords; **Inlets (waterways); Ocean currents;** Ocean engineering; **Oceanography;** Water transfer

ABSTRACT: As part of a comprehensive program of marine environmental studies in Port Valdez, Alaska, currents were measured in or near Valdez Narrows almost continuously for more than two years. The purpose of these measurements was to investigate the exchange of water between Port Valdez and Prince William Sound. Intensive profiling of temperature and salinity in Port Valdez and adjacent waters has enabled observation of water exchange processes that are effective on a seasonal basis. However, the current meter data have shown that these processes are occasionally overshadowed by short-term events that are of comparable effectiveness in promoting the exchange of water between Port Valdez and Prince William Sound. The latter events have typical durations of two to five days and their timing is apparently related to the passage of weather systems through the Gulf of Alaska. The random nature of these events, in conjunction with the generally predictable seasonal exchange processes, suggests that the notion of a unique residence time for Port Valdez and similar fjords is inappropriate.

REFERENCE: Colonell, Joseph M. (Senior Project Engr., Woodward-Clyde Consultants, Anchorage, Alaska 99503), "Deep Water Renewal in Subarctic Fjord," *Journal of the Waterway, Port, Coastal and Ocean Division*, ASCE, Vol. 107, No. WW4, **Proc. Paper 16632**, November, 1981, pp. 223-231

## 16674 LABORATORY INVESTIGATION OF EBB TIDAL SHOALS

KEY WORDS: **Inlets (waterways); Laboratory tests;** Models; **Sedimentation; Shoals;** Tidal traffic flow; Tides

ABSTRACT: The morphology of ebb tidal shoals has received considerable attention in the last few years, but no generally applicable techniques have evolved to predict shoal development. This engineering study is a first step in that direction. Shoals were generated in a laboratory basin and the basin controlling parameters were identified. Results indicate that the inlet behaves as a two dimensional turbulent jet and that inlet width, discharge velocity, and critical sediment velocity govern the equilibrium shoal dimensions. This preliminary study also suggests that the development of shoal length and width are governed by different transport mechanisms. Resolution of such possibilities requires more detailed studies.

REFERENCE: Sill, Ben L. (Assoc. Prof., Dept. of Civ. Engrg., Clemson Univ., Clemson, S. C.), Fisher, John S., and Whiteside, Stuart D., "Laboratory Investigation of Ebb Tidal Shoals," *Journal of the Waterway, Port, Coastal and Ocean Division*, ASCE, Vol. 107, No. WW4, **Proc. Paper 16674**, November, 1981, pp. 233-242

## U.S. Customary-SI Conversion Factors

In accordance with the October, 1970 action of the ASCE Board of Direction, which stated that all publications of the Society should list all measurements in both U.S. Customary and SI (International System) units, the following list contains conversion factors to enable readers to compute the SI unit values of measurements. A complete guide to the SI system and its use has been published by the American Society for Testing and Materials. Copies of this publication (ASTM E-380) can be purchased from ASCE at a price of $3.00 each; orders must be prepaid.

All authors of *Journal* papers are being asked to prepare their papers in this dual-unit format. To provide preliminary assistance to authors, the following list of conversion factors and guides are recommended by the ASCE Committee on Metrication.

| To convert | To | Multiply by |
|---|---|---|
| inches (in.) | millimeters (mm) | 25.4 |
| feet (ft) | meters (m) | 0.305 |
| yards (yd) | meters (m) | 0.914 |
| miles (miles) | kilometers (km) | 1.61 |
| square inches (sq in.) | square millimeters ($mm^2$) | 645 |
| square feet (sq ft) | square meters ($m^2$) | 0.093 |
| square yards (sq yd) | square meters ($m^2$) | 0.836 |
| square miles (sq miles) | square kilometers ($km^2$) | 2.59 |
| acres (acre) | hectares (ha) | 0.405 |
| cubic inches (cu in.) | cubic millimeters ($mm^3$) | 16,400 |
| cubic feet (cu ft) | cubic meters ($m^3$) | 0.028 |
| cubic yards (cu yd) | cubic meters ($m^3$) | 0.765 |
| pounds (lb) mass | kilograms (kg) | 0.453 |
| tons (ton) mass | kilograms (kg) | 907 |
| pound force (lbf) | newtons (N) | 4.45 |
| kilogram force (kgf) | newtons (N) | 9.81 |
| pounds per square foot (psf) | pascals (Pa) | 47.9 |
| pounds per square inch (psi) | kilopascals (kPa) | 6.89 |
| U.S. gallons (gal) | liters (L) | 3.79 |
| acre-feet (acre-ft) | cubic meters ($m^3$) | 1,233 |

# Deep Water Renewal in Subarctic Fjord

By Joseph M. Colonell,[1] M. ASCE

## Introduction

Port Valdez, Alaska, has gained prominence as the location of the marine terminal of the Trans-Alaska Pipeline System. As part of a comprehensive program of marine environmental studies of this subarctic fjord, currents were measured in Valdez Narrows for more than two years to examine the exchange of water between Port Valdez and Prince William Sound. These measurements have shown that flushing of Port Valdez is probably both frequent and intensive but the notion of a unique residence time for the fjord is inappropriate.

**Physical Oceanography of Port Valdez.**—Port Valdez and Valdez Arm form a 29 mi (46 km) northeasterly extension of Prince William Sound. Communication with the north Pacific Ocean is via Hinchinbrook Entrance, which opens on the Gulf of Alaska about 68 mi (110 km) from the town of Valdez (Fig. 1). The fjord of Port Valdez extends about 14 mi (23 km) eastward from Valdez Narrows, a narrow, double-silled entrance that is regarded as the demarcation between Port Valdez and Valdez Arm. The town of Valdez lies near the northeast corner of the fjord while the Trans-Alaska Pipeline System marine terminal is on the south shore at Jackson Point (Fig. 2).

Shaped somewhat like a bathtub, Port Valdez is about 3 mi (5 km) wide by 11 mi (18 km) long with steep sides on the north and south and a nearly horizontal bottom at a depth of about 790 ft (240 m) over three-quarters of its length. In the easternmost quarter of the fjord, the bottom rises rather uniformly to the eastern shore at the former townsite of Valdez. The maximum depth of Port Valdez is 810 ft (247 m), while the overall mean depth of the fjord is about 580 ft (180 m).

Port Valdez has an oceanographic regime that is strongly stratified (vertically) both in temperature and salinity during the summer months but is virtually unstratified during the winter months due to thermohaline convection (2,6). This fjord would be classified as a "positive" estuary since it receives more fresh water by runoff and precipitation than is lost through evaporation (1,2). This should imply that the classical estuarine circulation, with seaward movement of a brackish surface layer and landward movement of deeper waters, would

[1]Senior Project Engr., Woodward-Clyde Consultants, Anchorage, Alaska.

Note.—Discussion open until April 1, 1982. To extend the closing date one month, a written request must be filed with the Manager of Technical and Professional Publications, ASCE. Manuscript was submitted for review for possible publication on August 5, 1980. This paper is part of the Journal of the Waterway, Port, Coastal and Ocean Division, Proceedings of the American Society of Civil Engineers, ©ASCE, Vol. 107, No. WW4, November, 1981. ISSN 0148-9895/81/0004-0223/$01.00.

prevail in Port Valdez at least during periods of maximum runoff. Hydrographic data suggest that such flow does occur during the summer months but that it is confined to the top 50 ft (15 m) of the water column (2,6).

The tides in Port Valdez are of the mixed, semidiurnal type with a maximum

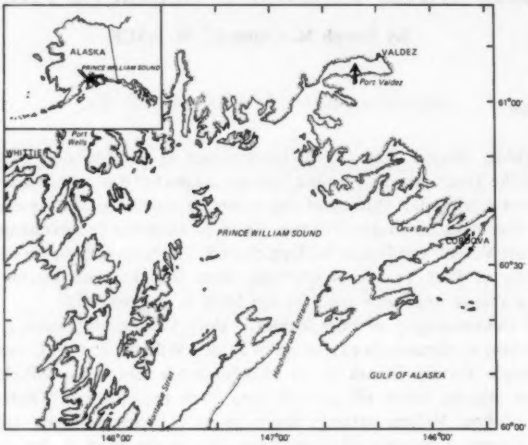


FIG. 1.—Location of Port Valdez

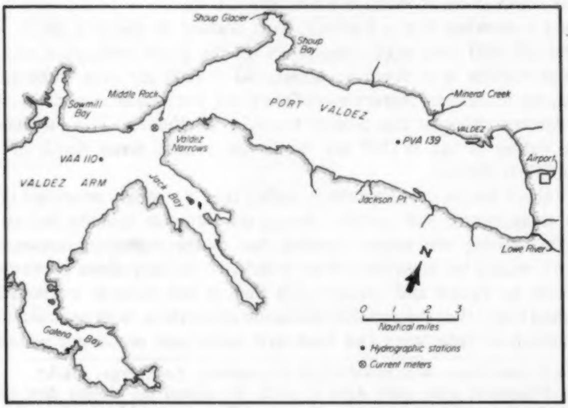


FIG. 2.—Map of Port Valdez

range of 17.5 ft (5.3 m) and a mean height of 10.0 ft (3.0 m). The tidal prism is about 1.6% of the total volume of Port Valdez (2). Assuming a homogeneous, well-mixed water body, i.e., winter conditions, it can be calculated that the

*half-life* of a volume of conservative substance is about 22 days in Port Valdez. This ignores any benefit of dilution by fresh water input, which would be negligible under winter conditions.

Just south of Valdez Narrows there are two sills, with maximum depth of 525 ft (160 m) that limit direct exchange of Port Valdez water below that depth with the deep waters of Prince William Sound. It should also be noted that direct exchange of water between the Sound and the Gulf of Alaska is similarly inhibited by a sill with maximum depth of about 574 ft (175 m) south of

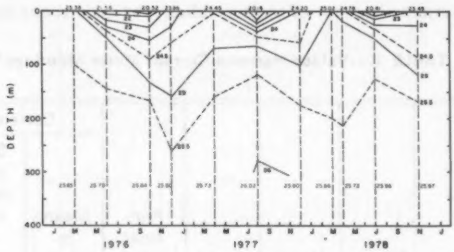


(a)

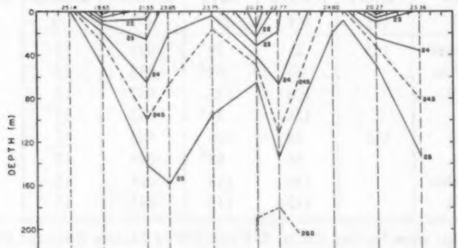


(b)

**FIG. 3.—Temporal Variation of Water Density ($\sigma_t$) at Hydrographic Stations: (*a*) Valdez Arm (VAA, upper); (*b*) Port Valdez (PVA 139, lower) $\sigma_t$ = (Specific Gravity − 1.00000) $\times 10^3$**

Hinchinbrook Entrance. Temporal variations of water density ($\sigma_t$) for one station within Port Valdez (PVA 139) and one in Valdez Arm (VAA 110) are presented as Fig. 3. These figures are essentially maps of the variation of water density with time. Each vertical dashed line corresponds to the density profile observed at the indicated time. The *contours* have been drawn simply by connecting points of equal density without attempting to smooth the data for a more realistic estimate of the variations between observations. Also, the difference in vertical scales should be noted.

Evidence of the intrusion of dense water from Prince William Sound into Valdez Arm and Port Valdez is apparent in Fig. 3. Appearing as pulses of increased density in mid-to-late summer, these annual intrusions serve to replenish bottom waters of several fjords in southcentral Alaska (5). The driving force for these intrusions has been attributed to the combined effects of prevailing winds over the Gulf of Alaska and the voluminous precipitation-runoff of the southcentral Alaska coastal region (8,9). During the summer and early autumn months, deep water exchange is enhanced by the development of classical estuarine flow conditions. The individual effectiveness of these processes is difficult to determine because of their simultaneous occurrence but a prior study

**TABLE 1.—Valdez Narrows Current Meter Moorings[a]**

| | | | | | | Current Speeds[b] | | |
|---|---|---|---|---|---|---|---|---|
| Mooring number (1) | Dates of deployment (2) | Water depth, in meters (3) | Meter depths, in meters (4) | Useful record, in days (5) | Principal axis of flow + *U* azimuth (6) | Mean, in centimeters per second (7) | Standard deviation, in centimeters per second (8) | Maximum, in centimeters per second (9) |
| VN-4 | December | 165 | 26 | 19[c] | 035 | 13 | 10 | 50 |
| | 8, 1977 to | | 63 | 62[c] | 038 | 11 | 8 | 48 |
| | April 19, | | 106 | 132 | 052 | 12 | 8 | 36 |
| | 1978 | | 156 | 34[c] | 035 | 11 | 8 | 36 |
| VN-5 | July 16, | 162 | 28 | 108 | 045 | 12 | 9 | 92 |
| | 1978 to | | 66 | 88[c] | 049 | 13 | 9 | 60 |
| | November | | 110 | 118 | 061 | 15 | 11 | 77 |
| | 11, 1978 | | 152 | 118 | 041 | 13 | 9 | 86 |

[a]Both moorings were located 0.6 mi (0.9 km) SW of Middle Rock (61.07° N, 146.66° W). Aanderaa RCM-4 current meters were used with data sampling interval set at 30 min.

[b]Computed from unfiltered data. VN-4 results are for data records truncated to 19-day period during which all four current meters were operating (December, 8–26, 1977)

[c]Short records due to battery failures.

of Port Valdez suggested residence times of approx 40 days (6).

**Valdez Narrows Currents.**—During the period from October, 1976–November, 1978, four long-term current meter moorings were placed in or near Valdez Narrows. The purpose of these moorings was to measure the exchange of water between Port Valdez and Prince William Sound. Although data from all four moorings have been examined, the most interesting and useful information has been derived from the two moorings that were deployed on the sill in Valdez Narrows (VN #4 and #5) at the location shown in Fig. 2. Some operational details for these moorings are provided in Table 1.

Current meter data were analyzed, first, in terms of true north-south and east-west components of the velocity vector. For data that are obtained in

a well-defined channel, such as Valdez Narrows, it is generally more useful to have the velocity vector resolved into its along-channel and cross-channel components. Rather than assume channel orientation from its appearance on a nautical chart, the statistics of the velocity data are used to obtain the preferred direction of flow, which is termed the "principal axis" of the flow (4). The latter is defined mathematically as that axis orientation for which the covariance of the velocity components is minimized. As shown in Table 1, the principal flow directions for the current meters in a single mooring tended to be quite

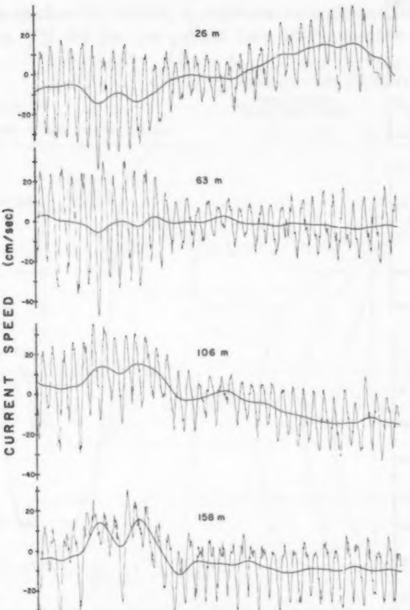


FIG. 4.—Along-Channel Velocity Component in Valdez Narrows (VN#4, 10–28 Dec., 1977). Positive Speed is Northeasterly Flow (Azimuth = 46°); Negative Speed is Southwesterly Flow (Azimuth = 226°). Unfiltered Signal is Shown as Fine Line; Dark Line is Net Speed after Removal of Tidal Constituents by Digital Filtering

similar, i.e. within a few degrees, so that an average angle for coordinate axis rotation was used to obtain the along-channel and cross-channel velocity components (termed $U$ and $V$, respectively) for all meters. Some statistics of observed current speeds are also listed in Table 1. All subsequent computations were performed on the velocity components as obtained for the principal axis orientation.

To obtain information on the net exchange of water through Valdez Narrows,

it was necessary to remove the tidal signal from the *raw* current meter data. A Butterworth low-pass filter was used for this purpose (7) with an example of the results (Fig. 4). In the latter figure both filtered and unfiltered data are displayed for the along-channel velocity component at each of four depths as obtained during December, 1977 (VN #4), showing how the *mean* flow is extracted from the total flow signal.

Because of battery failures in the current meters used in the VN #4 mooring,

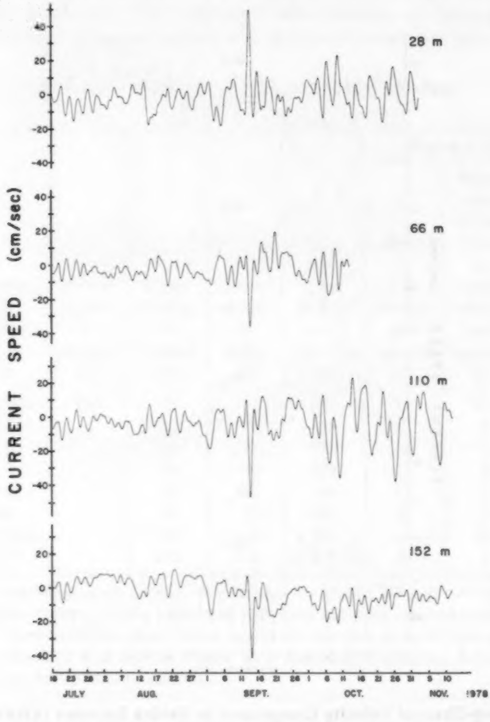


**FIG. 5.—Along-Channel Velocity Component in Valdez Narrows (VN#5, 18 July–10 November 1978). Positive Speed is Northeasterly Flow (Azimuth = 50°); Negative Speed is Southwesterly Flow (Azimuth = 230°)**

the period during which all four meters were operating was limited to December 10–28, 1977. As indicated by Table 1, useful data were obtained from other meters in this mooring for a longer period; however, it is sufficient for this discussion to focus on these shorter records. Referring to Fig. 4, two features are noteworthy. First, a *classical* estuarine flow is apparent during the period December 10–17, despite the fact that fresh water input is virtually zero at that time of year. Second, for the remainder of the record, the mean flow

profile is reversed with surface layer flow into Port Valdez and outward in the deeper layers. Weather data, consisting of winds at Middle Rock and daily mean barometric pressure at Valdez, were compared with the mean flow variations that are indicated by Fig. 4. It was concluded that the latter are not directly related to the local winds as measured at Middle Rock, but are fairly responsive to barometric pressure changes. This responsiveness was especially prominent for the period of December 12–16, when a two-lobed variation in current speed at all four meters coincided with a similar variation in barometric pressure (2).

In Fig. 5, the along-channel velocity components are plotted for all four current meters of mooring VN #5 for the period July 18–November 12, 1978. While

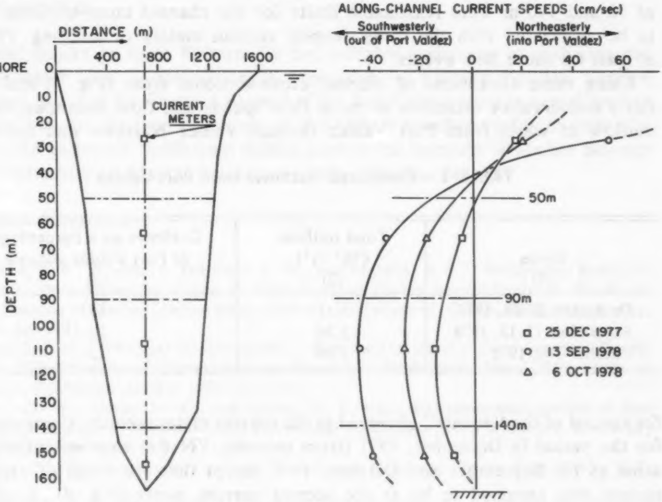


FIG. 6.—Cross-Section of Valdez Narrows, Showing Area Allocation to Current Meters for Flow Computations (Left); and Along-Channel Velocity Profiles (Net Speeds) Observed on Indicated Dates (Right)

occurrences of classical estuarine flow were definitely in evidence, as would be expected at that time of year, the prominent features of these records are the opposite flow conditions; that is, there were numerous occurrences of flow into Port Valdez in the surface layer with simultaneous outward flow in the deeper layers. While the "major event" of September 12–14 cannot escape notice, it should be noted that less spectacular but similar events occurred several times during the observation period. Attempts to correlate such events with available weather data were less satisfying than for the previous example and had to be regarded as inconclusive. Nevertheless, the hypothesis of a causal relationship between these events and the local or regional weather conditions is reasonable and warrants additional study. For purposes of this discussion,

however, it is sufficient to recognize the occurrence of these events and their probable relationship with weather patterns that are typical of southcentral Alaska. It remains to estimate the role of these events in promoting the exchange of water between Port Valdez and Prince William Sound.

Fig. 6 includes three examples of along-channel velocity profiles indicative of surface inflow-deep outflow events observed during December, 1977, and September and October of 1978. On the basis of these profiles, it was assumed that the depth of zero net motion was about 50 m. It should be emphasized that the indicated shapes of these velocity profiles are only estimates based on experience with a variety of flow phenomena; however, the profiles are probably satisfactory for the outflowing layer where the flow is reasonably well defined by observations at three depths. It was further assumed that depths of 90 and 140 m were reasonable limits for the channel cross-sectional areas to be associated with the three deepest current meters of mooring VN #5, at least for these flow events.

Using these allocations of channel cross-sectional areas (Fig. 6) and some fairly conservative estimates of mean flow speeds and flow durations, the net outflow of water from Port Valdez through Valdez Narrows was calculated for several of the "events" observed in the current meter records. Computations for the period in December, 1977 (from mooring VN #4) were essentially the same as for September and October, 1978 except that the depth of zero net motion was assumed to be at the second current meter (Fig. 4). Examples of the computed outflows are listed in Table 2. With magnitudes exceeding 15–20% of the volume of the fjord, it is apparent that only a few such events would be required to flush Port Valdez rather thoroughly.

**TABLE 2.—Computed Outflows from Port Valdez**

| Dates (1) | Total outflow ($10^9$ $m^3$) (2) | Outflows as a percentage of Port Valdez volume (3) |
|---|---|---|
| December 20–28, 1977 | 3.11 | 18 |
| September 13–15, 1978 | 3.76 | 22 |
| October 6–8, 1978 | 2.09 | 12 |

## Conclusions

Surges of surface water from Prince William Sound into Port Valdez, accompanied by large outflows from depths greater than 50–65 m, appear to be related to the passage of weather systems through southcentral Alaska. These events appear to be more effective in promoting deep water exchange than either tidal action or annual bottom water intrusions. Because of their apparent connection with atmospheric conditions, a certain degree of randomness is associated with these events so that a characteristic flushing rate is difficult to identify; however, the latter is probably a matter of no more than several days, in view of the large outflow volumes that were indicated by the current meter data.

The random nature of the weather-related events, in conjunction with the generally predictable seasonal and tidal exchange processes, implies that the notion of a unique residence time for Port Valdez is inappropriate. However, the observational evidence suggests that a conservative estimate of a composite residence time is probably no more than a few weeks. The latter depends, of course, on an assumption of reasonably uniform mixing throughout Port Valdez.

These conclusions should apply equally well to other fjords of southcentral Alaska, and perhaps to some in southeastern Alaska and northern British Columbia, since most are subject to the same meteorologic and oceanographic forcing functions.

## Acknowledgments

Special thanks go to Jo Roberts for her valuable assistance in analyzing the current meter data. Appreciation is expressed to Alyeska Pipeline Service Company, not only for financial support of the Port Valdez environmental studies program, but also for their insistence on the highest possible quality of scientific inquiry and endeavor. Additional thanks goes to the Institute of Marine Science at the University of Alaska, Fairbanks for Contribution No. 447.

## Appendix.—References

1. Carlson, R. F., Wagner, J., Hartman, C. W., and Murphy, R. S., "Freshwater Studies," *Baseline Data Survey for Valdez Pipeline Terminal Environmental Study*, D. W. Hood, ed., Institute of Marine Science Report R69-17, University of Alaska, Fairbanks, Alaska, 1969, pp. 7–41.
2. Colonell, J. M., "Physical Oceanography," *Port Valdez, Alaska: Environmental Studies 1976–1979*, Institute of Marine Science Occasional Publication, No. 5, University of Alaska, Fairbanks, Alaska, 1980, pp. 9–36.
3. Hood, D. W., Shiels, W. E., and Kelley, E. J., eds., *Environmental Studies of Port Valdez*, Institute of Marine Science Occasional Publication, Nos. 3 and 3A, University of Alaska, Fairbanks, Alaska, 1973.
4. Lumley, J. L., *Stochastic Tools in Turbulence*, Academic Press, New York, N.Y. 1970.
5. Muench, R. D., and Heggie, D. T., Deep Water Exchange in Alaskan Subarctic Fjords," *Estuarine Transport Processes*, B. Kjerfve, ed., University of South Carolina Press, Columbia, S.C., 1978.
6. Muench, R. D., and Nebert, D. L., Physical Oceanography, *Environmental Studies of Port Valdez*, D. W. Hood, W. E. Shiels and E. J. Kelley, eds., University of Alaska, Fairbanks, Alaska, 1973, pp. 103–149.
7. Roberts, J. and Roberts, T. D., "Use of the Butterworth Low-Pass Filter for Oceanographic Data, Journal of Geophysical Research, Vol. 83, No. 11, 1978, pp. 5510–5514.
8. Royer, T. C., "Seasonal Variations of Water in the Northern Gulf of Alaska," *Deep-Sea Research*, Vol. 22, 1975, pp. 403–416.
9. Royer, T. C., "On the Effect of Precipitation and Runoff on Coastal Circulation in the Gulf of Alaska," *Journal of Physical Oceanography*, Vol. 9, No. 3, 1979, pp. 555–563.

[illegible]

[illegible]

[illegible]

[illegible]

[illegible]

# Laboratory Investigation of Ebb Tidal Shoals

By Ben L. Sill,[1] John S. Fisher,[1] Members, ASCE,
and Stuart D. Whiteside,[2] A. M., ASCE

## Introduction

One of the dominant features of many tidal inlets is the ebb tidal shoal. Generally characterized by a horseshoe shape, this lobe of sediment often controls and in turn is controlled by the tidal currents and channels (5). The ebb tidal shoal is the zone of deposition for sediment carried by tidal currents from the interior bay or estuary and by longshore currents. The material moved in suspension and as bedload by the ebb discharge is deposited as the flow slows with increased depth, lateral spread, and mixing. In general, the size, geometry, and position of the shoal appear to depend on the texture of its sediment, strength of tidal and longshore currents, inlet morphology, and nearshore wave climate.

While significant work has been done on the morphology of ebb tidal shoals (5,2,6), little has been published on the relationship of this deposit to the controlling hydrodynamics. Ozsoy (7), Dean and Walton (4), and others have suggested both theoretical and experimental approaches, and those studies guided our own efforts. Many ebb tidal flows can be characterized as turbulent jets (9,7) which can be analyzed in a relatively straightforward manner, both theoretically and in the laboratory. We investigated the development of the ebb tidal shoal the sediments of which were deposited after transport by such a jet.

The mechanics of shoal formation is of profound interest to coastal engineers. The manipulation of inlet geometries and dredging of navigation channels are but two of many design problems which either directly or indirectly involve the ebb tidal shoal. In order to address these questions adequately, a predictive model for shoal formation is needed. Our study is intended to be a basic step in the development of this model. Using a small laboratory basin, ebb shoals were formed with a steady jet. Waves, reversing flows (flood tide), and sloping bottom were not studied, so our conclusions cannot be applied directly to actual inlets. Rather, this initial study (8) was designed to evaluate the appropriateness

[1]Assoc. Prof., Dept. of Civ. Engrg., Clemson Univ., Clemson, S.C.
[2]Research Asst., Dept. of Civ. Engrg., Clemson Univ., Clemson, S.C.

Note.—Discussion open until April 1, 1982. To extend the closing date one month, a written request must be filed with the Manager of Technical and Professional Publications, ASCE. Manuscript was submitted for review for possible publication on August 22, 1980. This paper is part of the Journal of the Waterway, Port, Coastal and Ocean Division, Proceedings of the American Society of Civil Engineers, ©ASCE, Vol. 107, No. WW4, November, 1981. ISSN 0148-9895/81/0004-0233/$01.00.

of the jet hypothesis in the laboratory model. Positive results from these initial experiments will provide a foundation for a more complete laboratory study.

## Test Description and Results

The 3.7 m × 3.7 m × 0.6 m model basin used in this investigation is shown by a schematic diagram in Fig. 1. Water was withdrawn through a perforated weir that served to minimize undesirable recirculation currents. The pump discharge flowed around the basin through a valve and flowmeter and then through gravel filters which eliminated ripples and waves and allowed smooth flow through the inlet. The width of the inlet was adjusted by changing the separation of two 1.9 cm thick partitions. Test inlet widths varied between 1.3 cm and 5.1 cm, water depths varied from 4.3 cm to 15.2 cm, and flow rates from $8 \times 10^{-5}$ $m^3/s$–$120 \times 10^{-5}$ $m^3/s$.

After the inlet geometry was adjusted, sediment was placed directly in front of the inlet in one of two ways. In one method, a mound (175 $cm^3$–350 $cm^3$) of sediment was placed in an area approximately 15 cm × 15 cm directly in front of the inlet. In the other method, the sediment was placed 0.3 cm thick over a 0.6 m wide by 0.9 m long area in front of the inlet. Duplicate tests showed that neither the amount of sediment nor method of placement affected

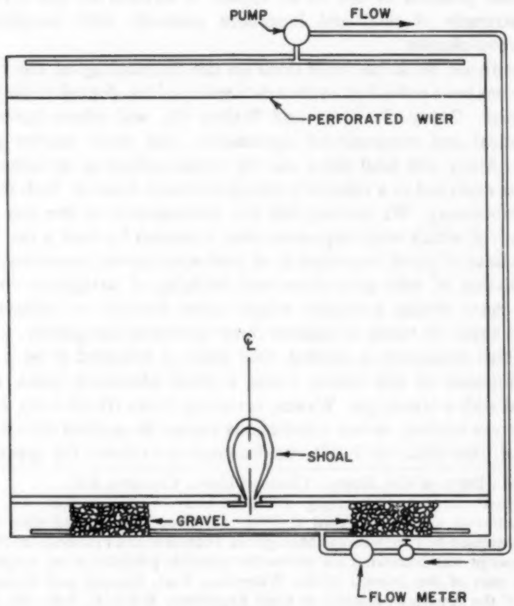


**FIG. 1.—Schematic Diagram of Model Basin Hydraulics Showing Developing Ebb-Tidal Shoal**

the results. During a test, the valve was adjusted to the desired flow rate, and the shoal was allowed to grow until a length change of no greater than

**TABLE 1.—Summary of Shoal Sediment Parameters**

| Sediment type (test numbers) (1) | Specific Gravity (2) | $d_{50}$, in millimeters $\times 10^3$ (3) | Critical velocity, in meters per second (4) | $\frac{u_c}{[gd_{50}(SG-1)]^{1/2}}$ (5) |
|---|---|---|---|---|
| Sand (1–18) | 2.65 | 500 | 0.17 | 1.86 |
| Sand (19) | 2.65 | 420 | 0.15 | 1.86 |
| Crushed walnut shells (20–26) | 1.30 | 700 | 0.12 | 2.54 |
| G-2 crushed glass (27–28) | 2.39 | 600 | 0.17 | 1.86 |
| Crushed brick (29–30) | 2.25 | 600 | 0.18 | 2.15 |

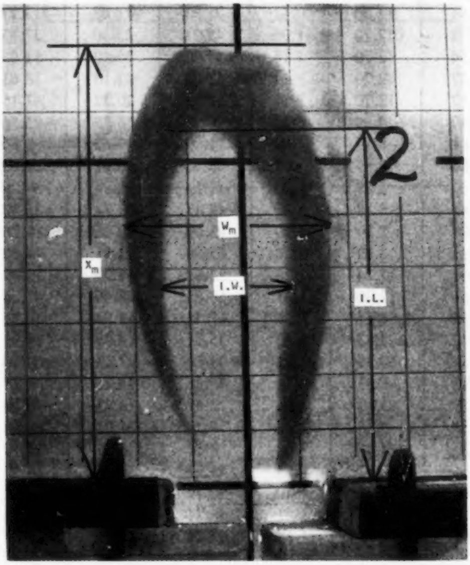


FIG. 2.—Locations of Important Dimensions on Shoals

one percent in one hour was achieved. The shape and size of the shoal (Fig. 2) was then photographed or diagrammed.

During the course of the test program, a total of thirty shoals were formed

from five sediment types of various particle sizes and specific gravities (Table 1). Steady-state shoal dimensions for the thirty tests are given in Table 2.

**TABLE 2.—Test Results**

| Test number (1) | Inlet width, in centimeters (2) | Water depth, in centimeters (3) | Flow rate, in cubic centimeters per millisecond (4) | Outside length, in centimeters (5) | Outside width, in centimeters (6) | Inside length, in centimeters (7) | Inside width, in centimeters (8) |
|---|---|---|---|---|---|---|---|
| 1 | 2.39 | 10.16 | 1.04 | 76.20 | 26.67 | 69.85 | 21.08 |
| 2 | 2.54 | 10.16 | .69 | 29.46 | 17.02 | 16.76 | 6.86 |
| 3 | 2.54 | 10.16 | .69 | 30.99 | 15.24 | 22.00 | 8.13 |
| 4 | 2.54 | 10.16 | .95 | 59.44 | 23.62 | 42.42 | 15.75 |
| 5 | 2.54 | 10.16 | 1.20 | 85.09 | 28.45 | 77.72 | 22.61 |
| 6 | 2.54 | 12.70 | .63 | 23.37 | 11.68 | 17.27 | 6.10 |
| 7 | 2.54 | 12.70 | 1.06 | 45.21 | 22.10 | 37.85 | 14.73 |
| 8 | 2.54 | 12.70 | 1.18 | 57.40 | 25.40 | 51.05 | 18.29 |
| 9 | 3.17 | 12.70 | 1.14 | 47.24 | 22.10 | 38.61 | 15.24 |
| 10 | 3.17 | 12.70 | 1.14 | 50.55 | 20.32 | 41.15 | 13.46 |
| 11 | 3.17 | 8.89 | 1.20 | 99.57 | 33.78 | 92.56 | 27.69 |
| 12 | 3.81 | 8.89 | .69 | 11.43 | 7.62 | 3.56 | 2.79 |
| 13 | 3.81 | 8.89 | .95 | 33.78 | 16.51 | 20.83 | 9.40 |
| 14 | 3.81 | 8.89 | 1.20 | 47.24 | 22.86 | 34.29 | 14.22 |
| 15 | 3.81 | 8.89 | 1.20 | 45.47 | 23.37 | 39.88 | 16.00 |
| 16 | 3.81 | 8.89 | 1.20 | 85.09 | 29.46 | 81.28 | 23.37 |
| 17 | 3.81 | 8.89 | 1.20 | 85.09 | 32.51 | 74.68 | 24.13 |
| 18 | 5.08 | 15.24 | 1.20 | 22.61 | 14.73 | 15.49 | 7.11 |
| 19 | 3.81 | 12.70 | 1.23 | 53.85 | 28.45 | 47.24 | 19.81 |
| 20 | 1.65 | 6.55 | .26 | 43.43 | 11.94 | 32.26 | 6.35 |
| 21 | 2.46 | 8.83 | .45 | 35.31 | 14.99 | 26.92 | 7.87 |
| 22 | 2.59 | 10.36 | .82 | 73.66 | 27.43 | 60.20 | 20.32 |
| 23 | 1.73 | 6.93 | .32 | 46.48 | 14.22 | 39.37 | 8.38 |
| 24 | 3.45 | 13.84 | 1.06 | 77.47 | 30.48 | 72.14 | 24.64 |
| 25 | 2.31 | 9.25 | .62 | 76.20 | 21.08 | 68.58 | 14.22 |
| 26 | 1.29 | 4.37 | .08 | 18.54 | 6.86 | 11.18 | 2.29 |
| 27 | 2.54 | 12.37 | .95 | 45.97 | 19.05 | 40.39 | 12.45 |
| 28 | 3.81 | 12.70 | 1.20 | 50.29 | 26.42 | 44.70 | 19.30 |
| 29 | 3.17 | 12.04 | 1.07 | 46.74 | 24.38 | 40.13 | 17.78 |
| 30 | 2.54 | 11.73 | 1.14 | 67.31 | 21.59 | 59.18 | 17.78 |

Regardless of the type of sediment or test situation, the classical horseshoe shape prevailed throughout the shoal formation.

## Analysis

For the thirty tests conducted, shoal dimensions varied substantially with sediment type, discharge velocity, $u_o$, inlet width, $W_i$, and depth, $D$. Pri

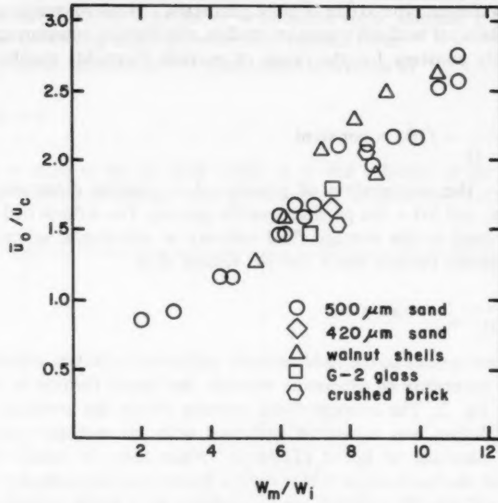


**FIG. 3.—Nondimensional Maximum Shoal Width Versus Nondimensional Initial Average Velocity for all Sediment Types**

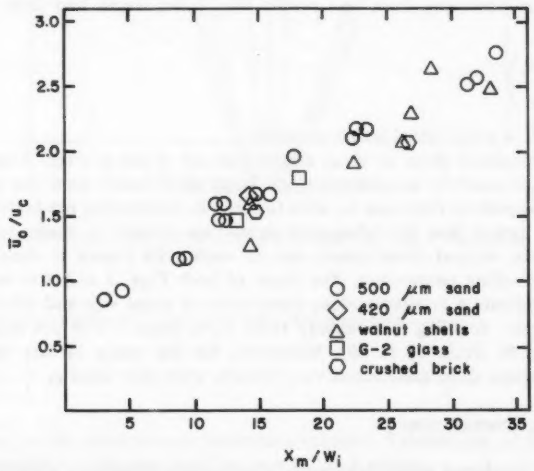


**FIG. 4.—Nondimensional Maximum Shoal Length Versus Nondimensional Initial Average Velocity for all Sediment Types**

to performing a dimensional analysis of the pertinent parameters, it was necessary to relate the sediment type to one or more geometric or hydrodynamic parameters.

Based on classical bedload transport studies, the Shields entrainment function, $F$, is relatively constant for the range of particle Reynolds numbers, $u_* d/\nu$, tested. Thus

$$F = \frac{u_*^2}{gd(SG - 1)} = f(\mathsf{R}) \simeq \text{constant} \quad \text{(1)}$$

in which $g$ = the acceleration of gravity; $d$ = particle diameter; $u_*$ = the shear velocity; and $SG$ = the particle specific gravity. For a fixed bed roughness, $u_*$ is proportional to the average fluid velocity at mid-depth, $u_c$ (measured by an electromagnetic current meter for this study), thus

$$\frac{u_c}{[gd_{50}(SG - 1)]^{1/2}} = \text{constant} \quad \text{(2)}$$

in which $u_c$ corresponds to the fluid velocity sufficient to initiate particle motion. It is a simple procedure to determine whether the shoals formed in the present study satisfy Eq. 2. The average fluid velocity above the terminal lobe of a shoal at equilibrium was measured and used with the sediment properties to calculate the constant of Eq. 2 (Table 1). While there is some variation, it is not large and the implication is that for the initial analysis sediment properties (of diameter and specific gravity) can be replaced by a single variable, $u_c$:

$$L = F(u_c, u_o, W_i, D) \quad \text{(3)}$$

Employing the Buckingham Pi Theorem, a dimensional analysis of Eq. 3 gives, after observing from test results that water depth had little effect on shoal size

$$\frac{L}{W_i} = f\left(\frac{u_o}{u_c}\right)$$

in which $L$ = either shoal length or width.

Nondimensional plots of shoal dimensions are given in Figs. 3 and 4. The ability to successfully normalize results from all 30 tests opens the possibility that studies such as these can be used to assist in formulating predictive models.

To the extent that the laboratory shoals are similar in shape to those at actual inlets, several observations can be made with regard to their response to the controlling parameters. The slope of both Figs. 3 and 4 is sufficiently small to indicate a relatively close correlation of shoal size and inlet velocity. For example, doubling the velocity ratio $u_o/u_c$ from 1.2 to 2.4 triples shoal length $X_m/W_i$ (from 10 to 30). Moreover, for the range of test conditions, the equilibrium shoal dimensions vary linearly with inlet velocity.

## Theoretical Considerations

Having developed actual laboratory shoals using conditions usually satisfied by one-dimensional (1-D) jet analysis, analytical and experimental results were compared. Since sediment movement is related to the bottom shear stress, which in turn is proportional to the jet velocity, it was assumed that isopleths of

shear stress which would likely correspond to shoal position could be approximated by jet isotachs. These isotachs were obtained from classical 1-D jet theory, based on the governing equation in control volume form.

Conservation of streamwise ($x$) momentum is written as

$$\frac{d}{dx}\int_0^b u^2\,dy = 0 \qquad (5)$$

in which $b = b(x)$ is the jet half width; $u$ = the velocity in the $x$ direction; and $y$ = the lateral coordinate. It is customary to assume that velocity profiles

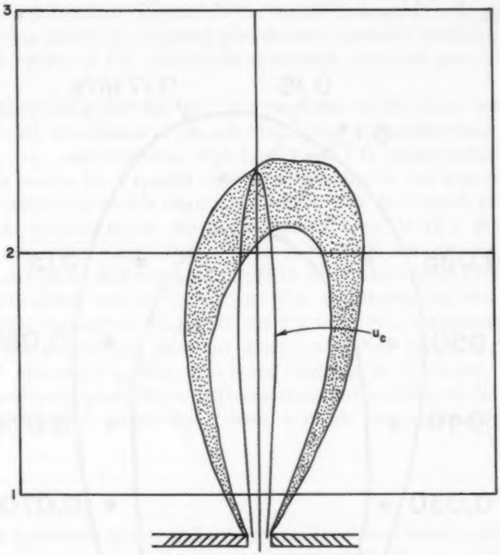


**FIG. 5.—Critical Velocity Isotach Shown with Shoal for Test 9 Plotted on 0.3 meter Square Grid**

exhibit dynamic similarity—our data also indicated this—or

$$\frac{u}{u_m} = F\left(\frac{y}{b}\right) \qquad (6)$$

in which $u_m$ = the maximum or centerline velocity. Substitution of Eq. 6 into Eq. 5, integration, and using $x = 0$, $u = u_0$, $b = b_0$ gives

$$u_m^2 bI = u_0^2 b_0 \qquad (7)$$

in which the constant

$$I = \int_0^1 f^2 d\left(\frac{y}{b}\right) \quad (8)$$

Our tests agreed with previous results (1) in that $b$ increases linearly with $x$ as

$$b = b_0 + C_j x \quad (9)$$

in which $C_j = 0.22$; and velocity profiles could be approximated by a cubic as

$$F = 1 - 3\left(\frac{y}{b}\right)^2 + 2\left(\frac{y}{b}\right)^3 \quad (10)$$

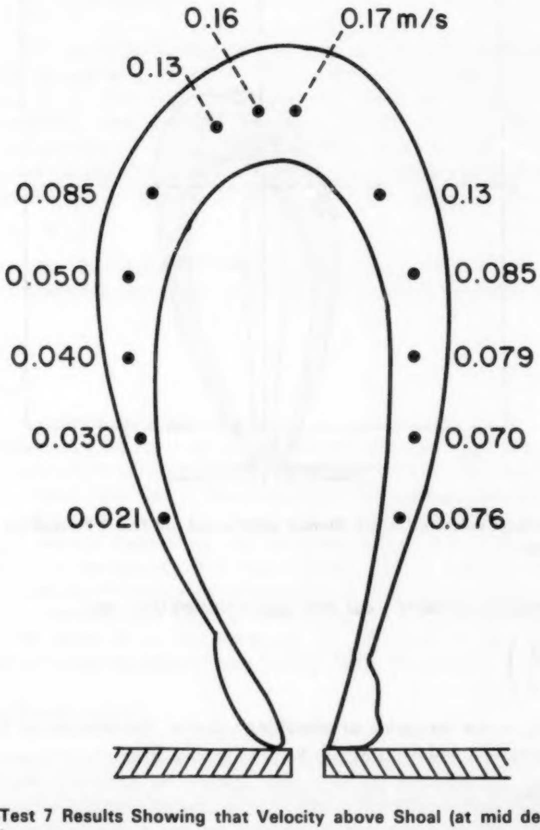


**FIG. 6.—Test 7 Results Showing that Velocity above Shoal (at mid depth) is not an Isotach**

As an overall check of the conformity of our inlet tests with accepted 1-D jet theory, Eq. 9 was substituted in Eq. 7, $u_m$ replaced by the critical velocity at the end of the shoal $u_c$, $x$ by $X_m$, the shoal length, and $I$ was calculated from

$$I = \frac{\left(\frac{u_o}{u_c}\right)^2}{\left(1 + \frac{C_j X_m}{b_o}\right)} \quad \text{(11)}$$

The average value of $I$ computed in this way from the first 24 tests was 0.32, as opposed to a theoretical value of 0.37 for Eq. 10. In summary, the jet discharges produced during this study exhibited growth rates, dynamic similarity of velocity profiles, and values of $I$ in reasonable agreement with that generally accepted for 1-D jets.

After demonstrating that the inlet jets produced in this study were basically one-dimensional, calculation of isotach shapes was straightforward. Eq. 10 was used with $u = u_c$, and combined with Eqs. 9 and 7 to obtain isotach locations. Fig. 5 shows results for a typical sand shoal. Results of this exercise indicated that all the laboratory shoals were much wider than the isotach corresponding to the critical velocity taken above the terminal lobe. In fact, the theoretical length-to-width ratios varied from 7.4 to 14.6, while the experimental ratios varied from 1.3 to 5.1 and averaged one-fifth of the theoretical values. Velocity measurements above one of the shoals (Fig. 6) substantiate this result—the shoal obviously was not an isotach. Ozsoy (7), using two-dimensional jet theory combined with a sediment transport model, predicted length to width ratios of about 10, also much greater than those observed in this study. The marked difference indicates a possibility of different transport mechanisms for the terminal lobe and the channel margin linear bars, a result also suggested by Butakov (3).

## Examination

All shoals generated during this study contained the characteristics generally attributed to those occurring in tide-dominated inlets. This was true regardless of the flow rate, inlet width, or sediment type used. The dimensions of the laboratory shoals were functions of inlet width, initial average velocity, and sediment type.

For this initial test program, the inlet width and "critical sediment velocity" were successfully used to normalize the relation between shoal size and discharge velocity. The resulting plots imply that some of the dominant parameters have been identified. The success of this analysis is encouraging and suggests that further research may permit the development of a truly predictive model.

To obtain a better understanding of the growth process, several 8 mm time-lapse movies were made of shoals from discharge initiation to their equilibrium position. Observations showed that the length to width ratio (aspect ratio) of shoals in their early growth phase was larger than the equilibrium value. For example, the aspect ratio of one shoal varied from 5.7 in the early stages of its development to 3.7 at its final equilbrium position. While these early aspect ratios were

higher than the previously mentioned 1.3–5.1 equilibrium values, they were still not as high as the theoretical values obtained from the isotach shape. More detailed studies are needed to determine if there is in fact a substantial difference in transport mechanisms on the channel margin linear bars and the terminal lobe.

Results of the test program and analysis can be summarized as follows:

1. Equilibrium shoal length and width increase in direct proportion to the average inlet velocity.
2. Inlet width and "critical" sediment velocity measured at mid-depth are appropriate scale factors for the laboratory shoals.
3. Two-dimensional theoretical isotach shape does not satisfactorily predict the equilibrium shoal shape.

More definitive conclusions await the generation of larger laboratory shoals which use a movable bed and include longshore currents and a sloping bottom.

## Appendix.—References

1. Abramovich, G. N., *The Theory of Turbulent Jets*, The Massachusetts Institute of Technology Press, Cambridge, Mass., 1963.
2. Boothroyd, J. C., "Mesotidal Inlets and Estuaries," *Coastal Sedimentary Environments*, R. A. Davis, Jr., ed., Springer-Verlag, N.Y., New York, 1978.
3. Butakov, A. N., "Study of Development and Deformation of Mouth Bar," Fourteenth Congress of the International Association for Hydraulic Research, Vol. 4, No. D-12, 1971, pp. 93–102.
4. Dean, R. G., and T. L. Walton, Jr., "Sediment Transport Processes in the Vicinity of Inlets with Special Reference to Sand Trapping," *Estuarine Research*, Vol. II: Geology and Engineering, L. E. Cronin, ed., Academic Press, New York, N.Y., 1975.
5. Hayes, M. O., and Kana, T. W., "Terrigenous Clastic Depositional Environments," *Technical Report No. 11-CRD*, Coastal Research Division, Dept. of Geology, University of South Carolina, 1978.
6. Nummendal, D., and Humphries, S. M., "Hydraulics and Dynamics of North Inlet. 1975–76," General Investigation of Tidal Inlets, *Report 10*, U.S. Army Coastal Engineering Research Center, 1978.
7. Ozsoy, E., "Flow and Mass Transport in the Vicinity of Tidal Inlets," *Report No. UFL/COEL/TR-036*, Coastal and Oceanographic Engineering Lab., University of Florida, 1977.
8. Whiteside, S. D., "A Laboratory Investigation of Shoaling Patterns of Tidal Inlets," thesis presented to Clemson University, at Clemson, South Carolina, in 1979, in partial fulfillment of the requirements for the degree of Master of Science, p. 62.
9. Wright, L. D., and J. M. Coleman, "Mississippi River Mouth Processes: Effluent Dynamics and Morphologic Development," *Journal of Geology*, Vol. 82, 1974, pp. 751–778.

# TECHNICAL NOTES

Note.—Discussion open until April 1, 1982. To extend the closing date one month, a written request must be filed with the Manager of Technical and Professional Publications, ASCE. This paper is part of the Journal of the Waterway, Port, Coastal and Ocean Division, Proceedings of the American Society of Civil Engineers, ©ASCE, Vol. 107, No. WW4, November, 1981.

# Technical Notes

To provide a place within ASCE for publication of technical ideas that have not advanced, as yet, to the point where they warrant publication as a Proceedings paper in a *Journal*, the publication of Technical Notes was authorized by the Board of Direction on October 16–18, 1967, under the following guidelines:

1. An original manuscript and two copies are to be submitted to the Manager of Technical and Professional Publications, ASCE, 345 East 47th Street, New York, N.Y., 10017, along with a request by the author that it be considered as a Technical Note.
2. The two copies will be sent to an appropriate Technical Division or Council for review.
3. If the Division or Council approves the contribution for publication, it shall be returned to Society Headquarters with appropriate comments.
4. The technical publications staff will prepare the material for use in the earliest possible issue of the *Journal*, after proper coordination with the author.
5. Each Technical Note is not to exceed 4 pages in the *Journal*. As an approximation, each full manuscript page of text, tables, or figures is the equivalent of one-half a *Journal* page.
6. The Technical Notes will be grouped in a special section of each *Journal*.
7. Information retrieval abstracts and key words will be unnecessary for Technical Notes.
8. The final date on which a Discussion should reach the Society is given as a footnote with each Technical Note.
9. Technical Notes will not be included in *Transactions*.
10. Technical Notes will be included in ASCE's annual and cumulative subject and author indexes.

The manuscripts for Technical Notes must meet the following requirements:

1. Titles must have a length not exceeding 50 characters and spaces.
2. The author's full name, Society membership grade, and a footnote reference stating present employment must appear on the first page of the manuscript. Authors need not be Society members.
3. The manuscript is to be submitted as an original copy (with two duplicates) that is typed double-spaced on one side of 8-1/2-in. (220-mm) by 11-in. (280-mm) white bond paper.
4. All mathematics must be typewritten and special symbols must be properly identified. The letter symbols used must be defined where they first appear, in figures or text, and arranged alphabetically in an Appendix.—Notation.
5. Standard definitions and symbols must be used. Reference must be made to the lists published by the American National Standards Institute and to the *Authors' Guide to the Publications of ASCE*.
6. Tables must be typed double-spaced (an original ribbon copy and two duplicate copies) on one side of 8-1/2-in. (220-mm) by 11-in. (280-mm) paper. An explanation of each table must appear in the text.
7. Figures must be drawn in black ink on one side of 8-1/2-in. (220-mm) by 11-in. (280-mm) paper. Because figures will be reproduced with a width of between 3 in. (76 mm) to 4-1/2 in. (110 mm), the lettering must be large enough to be legible at this width. Photographs must be submitted as glossy prints. Explanations and descriptions must be made within the text for each figure.
8. References cited in text must be typed at the end of the Technical Note in alphabetical order in an Appendix.—References.
9. Dual units, i.e., U.S. Customary followed by SI (International System) units in parentheses, should be used throughout the paper.

# Bottom Smoothing to Prevent Numerical Instability

By Fred E. Camfield,[1] M. ASCE

## Introduction

Numerical simulation of sediment transport and the changes in plan form of the shoreline near coastal structures may produce results where the bottom slope exceeds the maximum slope which would be expected to occur on the real (prototype) shoreline. This may cause an instability in the numerical solution and prevent an accurate simulation of the transport processes. A numerical subroutine has been developed to redistribute the sediment at points where the numerically produced bottom slope exceeds the maximum expected slope. This subroutine has no dependence on time. The smoothing is accomplished numerically after the completion of one or more iterations of time-dependent, numerical simulation of physical processes, e.g., sediment transport associated with wave action or currents. It should be noted that the smoothing subroutine will smooth any input data to reach a maximum slope between points, even random numbers. This subroutine should not be used as a substitute for good simulation of the physical processes, but may be used to smooth errors resulting from the inexact nature of numerical modeling.

## Numerical Subroutine

It is assumed here that a rectangular array is used for the numerical computation. The results presented can be modified for cases where a rectangular array is not used, e.g., near a boundary. A nine-point rectangular array is used for the computations at each grid point (Fig. 1). The water depths are expressed as positive numbers for ease of computation.

The first step in the computation is the determination of potential sediment movement, $\delta$, between point $(x_j, y_k)$ at the center of the array and each of the surrounding points. A difference in depth, which would result in a maximum slope, $S_m$, expected to occur between the two points for the known physical conditions, is compared with the difference in depth produced by the numerical simulation of the physical processes moving the sediment. This gives

[1]Hydr. Engr., U.S. Army Coastal Engrg. Research Center, Kingman Bldg., Ft. Belvoir, Va. 22060.

Note.—Discussion open until April 1, 1982. To extend the closing date one month, a written request must be filed with the Manager of Technical and Professional Publications, ASCE. Manuscript was submitted for review for possible publication on September 17, 1980. This paper is part of the Journal of the Waterway, Port, Coastal and Ocean Division, Proceedings of the American Society of Civil Engineers, ©ASCE, Vol. 107, No. WW4, November, 1981. ISSN 0148-9895/81/0004-0245/$01.00.

$$\delta_i = \frac{|D_1 - D_i| - S_m r_i}{2} \quad \ldots \ldots \ldots \ldots \ldots \quad (1)$$

in which $D_1$ = the water depth at the point $(x_j, y_k)$, $D_i$ the water depth at another point in the array, and $r_i$, the distance between the two points, given as

$$r_i = \Delta y, \quad \text{at} \quad (x_j, y_{k+1}), \quad (x_j, y_{k-1}) \quad \ldots \ldots \quad (2)$$

$$r_i = \Delta x, \quad \text{at} \quad (x_{j+1}, Y_k), \quad (x_{j-1}, y_k) \quad \ldots \ldots \quad (3)$$

$$r_i = [(\Delta x)^2 + (\Delta y)^2]^{1/2}, \quad \text{at} \quad (x_{j-1}, y_{k+1}); \quad (x_{j+1}, y_{k+1});$$

$$(x_{j-1}, y_{k-1}); \quad (x_{j+1}, y_{k-1}) \quad \ldots \ldots \quad (4)$$

Where $\delta_i \leq 0$, no sediment motion is assumed to occur, and $\delta$ is set equal

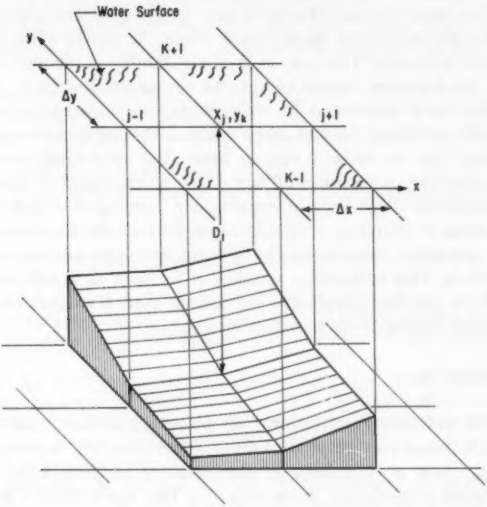


**FIG. 1.—Nine-Point Rectangular Array and Representation of Sea Bottom for Numerical Computation**

to zero at those points. After considering all surrounding points and setting $\delta_i = 0$ where no motion would occur, the direction of potential motion to and from the remaining points must be determined. This is shown by

$$\nu_i = -\delta_i; \quad D_i > D_1 \quad \ldots \ldots \quad (5)$$

which converts $\delta_i$ to a negative number, $\nu_i$, where $D_i > D_1$, i.e., where the potential sediment movement is away from the center of the array.

It is then necessary to determine the interrelationships of the potential sediment motions. This is done by first expressing the potential sediment motions in terms of their relative influence

$$\delta_i' = \frac{\delta_i}{r_i} \quad \text{(6)}$$

and $$\nu_i' = \frac{\nu_i}{r_i} \quad \text{(7)}$$

Next, the total sums of the positive and negative potential sediment movements, $\Sigma\delta_i'$ and $\Sigma\nu_i'$, are expressed in terms of equivalent numbers of maximum poten-

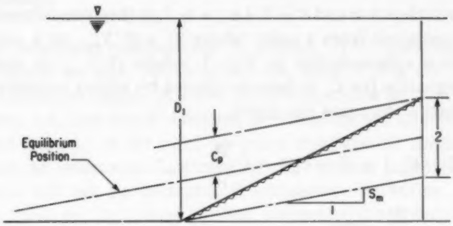


FIG. 2.—Schematic of Depth Correction, $\Sigma\nu_i = 0$

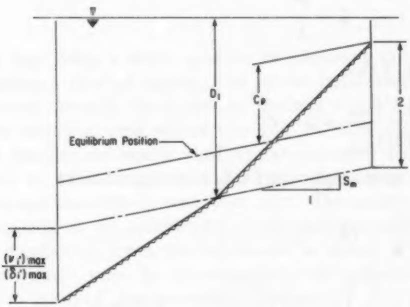


FIG. 3.—Schematic of Depth Correction

tials, $(\delta_i')_{max}$ and $(\nu_i')_{max}$, respectively, so that

$$p = \frac{\Sigma\delta_i'}{(\delta_i')_{max}} \quad \text{(8)}$$

and $$n = \frac{\Sigma\nu_i'}{(\nu_i')_{max}} \quad \text{(9)}$$

To determine correction coefficients, $c_p$ and $c_n$, to correct the positive and negative potential sediment movements, $\delta_i$'s and $\nu_i$'s, respectively, the case in which $\Sigma\nu_i = 0$ is considered first. In Fig. 2, where $(\delta_i')_{max}$ has been normalized to unity, i.e., where $(\delta_i')_{max}$ is represented by a unit quantity,

(increase at center) = (decrease at exterior points)

$$(2 - C_p) = C_p p, \quad \Sigma \nu_i = 0 \quad (10)$$

which gives $C_p = \dfrac{2}{p+1}, \quad \Sigma \nu_i = 0$ (11)

Similarly, in cases in which $\Sigma\delta_i = 0$

$$C_n = \frac{2}{n+1}, \quad \Sigma \delta_i = 0 \quad (12)$$

The case in which $p \geq n$ and $n \neq 0$, i.e., $n \geq 1$, is then considered. The potential movement of sediment from a point where $\delta_i' = (\delta_i')_{\max}$ to a point where $\nu_i' = (\nu_i')_{\max}$ is shown schematically in Fig. 3, where $(\delta_i')_{\max}$ is again normalized to unity. The equation for $C_p$ is then developed by noting increase (on left) + increase (at center) = decrease (on right)

$$\left(\frac{2|\nu_i'|_{\max}}{(\delta_i')_{\max}} + 2 - C_p\right) + (2 - C_p) = C_p \frac{p}{n} \quad (13)$$

which gives $C_p = \dfrac{\dfrac{2|\nu_i'|_{\max}}{(\delta_i')_{\max}} + 4}{2 + \dfrac{p}{n}}, \quad p \geq n \geq 1$ (14)

Noting from Fig. 3 that

$$C_n \frac{|\nu_i'|_{\max}}{(\delta_i')_{\max}} = 2\frac{|\nu_i'|_{\max}}{(\delta_i')_{\max}} + 2 - C_p \quad (15)$$

and substituting on the right-hand side from equation 13

$$C_n \frac{|\nu_i'|_{\max}}{(\delta_i')_{\max}} = C_p \frac{p}{n} - (2 - C_p) \quad (16)$$

then $C_n = \left[\left(1 + \dfrac{p}{n}\right) C_p - 2\right] \dfrac{(\delta_i')_{\max}}{|\nu_i'|_{\max}}, \quad p \geq n \geq 1$ (17)

Similarly, it can be seen that for cases in which $n > p$ and $p \geq 1$,

$$C_n = \frac{\dfrac{2(\delta_i')_{\max}}{|\nu_i'|_{\max}} + 4}{2 + \dfrac{n}{p}}, \quad n \geq p \geq 1 \quad (18)$$

and $C_p = \left[\left(1 + \dfrac{n}{p}\right) C_n + 2\right] \dfrac{|\nu_i'|_{\max}}{(\delta_i')_{\max}}, \quad n \geq p \geq 1$ (19)

Using the appropriate values of $C_p$ and $C_n$, it is now possible to correct the depths in the array. For cases in which $D_i < D_1$ and $\delta_i > 0$

$$D_i' = D_i + C_p \delta_i, \quad \delta_i > 0 \quad (20)$$

$D'_i$ is the corrected depth. For cases in which $D_i > D_1$ and $\delta_i > 0$, from Eq. 5, $\nu_i = -\delta_i$,

$$D'_i = D_i + C_n \nu_i \qquad (21)$$

(remembering that $\nu_i$ has a negative value). From conservation of mass

$$D'_1 = D_1 - C_p \Sigma \delta_i - C_n \Sigma \nu_i \qquad (22)$$

## Adjusted Coefficients

Because the numerical computation is inexact, it is necessary to consider how the corrections in Eqs. 20–22 affect the data. Using the full correction shown in the equations might, in some instances, cause an "over correction" to the input data; i.e., too much sediment is moved by the numerical subroutine at a given point because of the point-by-point computation through the matrix. This may cause an excessive flattening of the bottom slope (to a slope less than $S_m$), which will not be corrected in successive iterations. This could be partly compensated for by using smaller correction coefficients, $C'_p$ and $C'_n$, given as

$$C'_p = \alpha C_p \qquad (23)$$

and $$C'_n = \alpha C_n \qquad (24)$$

in which $\alpha < 1.0$, and using a larger number of iterations through the matrix. This was tested using a $15 \times 20$ matrix. Use of the full-correction coefficients required 12 iterations through the matrix to reach a solution. Where $\alpha = 0.6$, 18 iterations were required, and where $\alpha = 0.3$, 28 iterations were required. While use of the smaller correction coefficients provided some improvement in the final values of water depth at individual points, this was offset by a substantial percentage increase in computer time. The actual cost increase in computer time depends on the complexity of the problem where the subroutine is used, and the number of times the subroutine is called. The desirability of using smaller coefficients must be determined by the individual programer. If smaller coefficients are used, the necessary condition is

$$\frac{C'_p}{C'_n} = \frac{C_p}{C_n} \qquad (25)$$

It has been assumed that no sediment motion will occur at points in which $(|D_1 - D_n| - S_m r) < 0$. This would not be true if $|D'_1 - D_n| - S_m r) > 0$. However, no attempt is made here to account for this additional sediment motion. Direct computation at each grid point in the network would require a significant increase in computational time, i.e., recomputing depth differences and readjusting depths through a number of iterations, and the smoothing computations from point-to-point plus successive iterations through the entire network should account for the resulting motion.

## Acknowledgment

The results presented in this paper are based on research conducted at the

Coastal Engineering Research Center under the Coastal Engineering Research Program of the U.S. Army Corps of Engineers. Permission to publish this information is appreciated.

# DISCUSSION

Note.—This paper is part of the Journal of the Waterway, Port, Coastal and Ocean Division, Proceedings of the American Society of Civil Engineers, ©ASCE, Vol. 107, No. WW4, November, 1981. ISSN 0148-9895/81/0004-0253/$01.00.

# Discussions

Discussions may be submitted on any Proceedings paper or technical note published in any *Journal* or on any paper presented at any Specialty Conference or other meeting, the *Proceedings* of which have been published by ASCE. Discussion of a paper/technical note is open to anyone who has significant comments or questions regarding the content of the paper/technical note. Discussions are accepted for a period of 4 months following the date of publication of a paper/technical note and they should be sent to the Manager of Technical and Professional Publications, ASCE, 345 East 47th Street, New York, N.Y. 10017. The discussion period may be extended by a written request from a discusser.

The original and three copies of the Discussion should be submitted on 8-1/2-in. (220-mm) by 11-in. (280-mm) white bond paper, typed double-spaced with wide margins. The length of a Discussion is restricted to two *Journal* pages (about four typewritten double-spaced pages of manuscript including figures and tables); the editors will delete matter extraneous to the subject under discussion. If a Discussion is over two pages long it will be returned for shortening. All Discussions will be reviewed by the editors and the Division's or Council's Publications Committees. In some cases, Discussions will be returned to discussers for rewriting, or they may be encouraged to submit a paper or technical note rather than a Discussion.

Standards for Discussions are the same as those for Proceedings Papers. A Discussion is subject to rejection if it contains matter readily found elsewhere, advocates special interests, is carelessly prepared, controverts established fact, is purely speculative, introduces personalities, or is foreign to the purposes of the Society. All Discussions should be written in the third person, and the discusser should use the term "the writer" when referring to himself. The author of the original paper/technical note is referred to as "the author."

Discussions have a specific format. The title of the original paper/technical note appears at the top of the first page with a superscript that corresponds to a footnote indicating the month, year, author(s), and number of the original paper/technical note. The discusser's full name should be indicated below the title (see Discussions herein as an example) together with his ASCE membership grade (if applicable).

The discusser's title, company affiliation, and business address should appear on the first page of the manuscript, along with the *Proceedings* paper number of the original paper/technical note, the date and name of the *Journal* in which it appeared, and the original author's name.

Note that the discusser's identification footnote should follow consecutively from the original paper/technical note. If the paper/technical note under discussion contained footnote numbers 1 and 2, the first Discussion would begin with footnote 3, and subsequent Discussions would continue in sequence.

Figures supplied by the discusser should be designated by letters, starting with A. This also applies separately to tables and references. In referring to a figure, table, or reference that appeared in the original paper/technical note use the same number used in the original.

It is suggested that potential discussers request a copy of the *ASCE Authors' Guide to the Publications of ASCE* for more detailed information on preparation and submission of manuscripts.

# INLINE FORCES ON FIXED VERTICAL CYLINDERS IN WAVES[a]

Closure by Subrata K. Chakrabarti,[4] F. ASCE

The discussions of Ramberg and Christodoulou are appreciated.

There seems to be some confusion regarding the data reduction procedure adopted in the paper. A test record typically was ten cycles long. Irregular stream function theory was used to predict the water particle kinematics from the wave profile. Each cycle of the profile was fitted with the theory and the water particle velocity and acceleration profiles were derived from it. Since there was some variation of the wave profile from one cycle to the next, the values of the kinematics, e.g., $u_m$ were different from cycle to cycle. However, the variation of these values was generally small and account for the clustering of the data points in Fig. 3. These variations in the $C_M$ and $C_D$ values within one wave record were much greater than any errors in the measurement. In the absence of the measured kinematics of the flow field near the cylinder it is difficult to attribute the cause of the variations to a physical factor. However, it is possible that the flow field in the vicinity of the cylinder is constantly changing due to change in the vortex shedding process from the cycle to cycle variation in the free surface profile. This, in turn, alters the values of $C_M$ and $C_D$. In a controlled planar harmonic flow (e.g. Sarpkaya's experiment) such cycle to cycle variation is avoided.

Regarding comparison of the hydrodynamic coefficients from the wave tank test with those from the planar flow results, it should be noted that only the mean values of data were used. Referring to Fig. 3, it may be seen that the spread in the data, particularly in the $C_D$ values, is large. In the lower end of the envelope, the $C_D$ values are appreciably lower than Sarpkaya's results, while the upper end values are higher. Ramberg's (13) comparison was made only with eight data points and cannot be called conclusive. Moreover, his data were averaged over the length of the vertical cylinder (since total forces were measured) and his discussion applied to a range of KC values where the drag force contribution is quite small compared with the inertia force contribution and, as such, is amenable to substantial error. For example, if the drag force is about 10% of the total force, a 2% error in the measurement may produce a large error in the computed drag coefficient. The writer agrees with Ramberg's explanation of the variation of the two results as partly contributing to the three-dimensionality of the flow field and different kinematic gradients due to orbital variation.

It should be further noted that in an experiment with a vertical cylinder, the coefficients should be based on the measured force data from a small segment of the cylinder. Any conclusion derived from averaged values over the length

---

[a] May, 1980, by Subrata K. Chakrabarti (Proc. Paper 15403).

[4] Dir., Marine Research and Development, Chicago Bridge & Iron Co., Plainfield, Ill.

of the cylinder is influenced by the averaging of the complex three-dimensional flow field.

Regarding the discussion of Christodoulou, it is, indeed, difficult to reach any fruitful conclusions regarding the influence of $R$ on $C_M$ and $C_D$ from the present study. This is primarily due to the small range of $R$. While the correlation between the results from the wave-flow here and the two-dimensional harmonic flow for the appropriate values of $R$ may be termed fair, the difference is still large, especially in view of the scatter in the $C_M$ and $C_D$ data. A more controlled experiment in a wave tank with a larger variation in $R$ is needed for the verification of these results. This, however, is extremely difficult to do because of the limitation of wave generation in the test facility. On the other hand, field test data are difficult to reliably obtain and their results difficult to interpret, due to additional environmental effects on the test cylinder.

The writer agrees with Christodoulou that the correlation of the total forces using data from the local forces on the same test cylinders is somewhat biased. Nonetheless, it establishes the accuracy of the measuring instruments since two types of instruments were used in measuring the total and local forces and the local forces are much more delicate to measure. Since more than one test cylinder and test set-up was used, it provides greater confidence in the data. It also determines the appropriateness and usefulness of the mean curves for $C_M$ and $C_D$ through a large scatter of data. The correlation of forces for the 1.5 in. diameter tube (Fig. 6) is poorer, not because it contributed fewer points, but because the computation applied the mean curves in the higher range of KC where data are sparse and subject to larger error. It would be worthwhile to correlate the data using results derived from other independent tests.

---

## Prediction of Extreme Wave Heights and Wind Velocities[a]

### Errata

The following corrections should be made to the original paper:

Page 474, line 5: Should read "$X = -\ln\left[-\ln\left(1 + \frac{1}{\lambda}\ln R\right)\right] \ldots (14)$" instead of "$X = -\ln\left[-\ln\left(1 + \frac{1}{\lambda}\ln\right)R\right] \ldots (14)$"

Page 475, line 3: Should read "$H_R = U + X_R\alpha$" instead of "$H_R = U + X_R$"

[a]November, 1980, by Liu Teh-fu and Ma Feng-shi (Proc. Paper 15862).

C 20